An Enhanced $0.8V_{OC}$-model-based Global Maximum Power Point Tracking Method for Photovoltaic Systems

Ziqiang Bi, *Student Member, IEEE,* Jieming Ma, *Member, IEEE,* Ka Lok Man, Jeremy S. Smith, Yong Yue, and Huiqing Wen, *Senior Member, IEEE*

***Abstract*—Under partial shading conditions (PSC), the power-voltage (P-V) characteristic curve of a photovoltaic (PV) string exhibits multiple peaks, posing a big challenge to the problem of global maximum power point tracking (GMPPT). The traditional $0.8V_{OC}$-model-based GMPPT method locates the global maximum power point (GMPP) locus by comparing the power at each local power peaks. However, a considerable amount of time is required for iteratively scanning each $0.8V_{OC}$ vicinity. To address this problem, an improved $0.8V_{OC}$-model-based GMPPT method is proposed in this paper. A shading vector is firstly used to characterize the PSC. The proposed GMPPT method estimates the $0.8V_{OC}$ region with the GMPP directly from the measured shading vector by the k-Nearest Neighbors (k-NN) approach and saves the time consumed in the comparison process involved in the conventional method. The simulation and experimental experiments demonstrate that the proposed method is capable of tracking the GMPP efficiently and accurately under various shading patterns. By comparing with the original $0.8V_{OC}$-model-based method, the proposed method reduces the tracking step by 75% while maintaining good prediction accuracy.**

***Index Terms*—Photovoltaic, maximum power point tracking, $0.8V_{OC}$ model, k-nearest neighbors, partial shading conditions.**

I. Introduction

NOWADAYS, due to the environmental concerns about global warming all over the world, the demand for renewable energy resources is increasing year by year. Solar energy is one of the most popular renewable energy resources since its noiseless and environmental-friendly power-generating process. Photovoltaic (PV) is the technology for converting solar energy to the electricity using semiconducting materials [1]. In PV systems, the existence of the partial shading is inevitable when part of the PV modules are shaded by the nearby buildings, trees or passing clouds. Under partial shading conditions (PSC), multiple stairs are presented on the current-voltage (I-V) characteristic curve of the PV system as a result, the power-voltage (P-V) characteristic curve exhibits multiple peaks [2]. The conventional maximum power point tracking (MPPT) methods based on simple searching techniques gradually search for the peak in the P-V curve. The most typical ones are perturb and observe (P&O) [3] and incremental conductance (IncCond) [4]. The wrong selection of the initial searching point may result in the local maximum power point (LMPP) instead of the global maximum power point (GMPP) [5]. Therefore, the capability of searching for the GMPP is critical for a global maximum power point tracking (GMPPT) system.

In order to track the GMPP, a method based on the full scanning technique was proposed in [6]. This method takes advantage of its simplicity because it blindly scans the whole P-V curve. However, the tracking performance is highly dependent on the scanning step. With a smaller scanning step, the system can track the precise GMPP but the scanning procedure is longer. With a larger scanning step, the scanning speed is faster but the system may overlook the GMPP.

The $0.8V_{OC}$ model originated from the work in [7] and [8] has shown that all the peaks in the P-V characteristic curve are occurring at the integer multiples of 80% of open-circuit voltage ($0.8V_{OC}$). Compared with the full scanning technique in [6], only the vicinities of the $0.8V_{OC}$ are scanned, and as a result, the scanning time is significantly reduced. A comparative study was conducted in [9] between the conventional P&O, the full scanning technique and a $0.8V_{OC}$-model-based method. The comparative results showed that under some shading patterns, the P&O technique is trapped at the LMPPs. The full scanning method tracks the GMPP accurately but the convergence time is significant. The GMPP is not guaranteed to be tracked by the $0.8V_{OC}$-model-based method, while compared with the full scanning technique, the tracking speed is largely improved [9].

In recent years, a number of $0.8V_{OC}$-model-based MPPT methods have been proposed [5], [10]–[16]. In [10], a new hybrid GMPPT algorithm containing an improved $0.8V_{OC}$-model-based approach with a smart power scanning procedure was proposed. The tracking efficiency has been improved up to 11.29% compared with the technique which monitors voltage and current variations. Limited and adaptive scanning approaches were proposed to improve the $0.8V_{OC}$ model [5], [12], [13]. The scanning ranges of the duty cycle for each $0.8V_{OC}$ region are generated from the PV parameters. By scanning the generated duty cycle ranges, this approach avoids

Z. Bi, J. Ma, K. L. Man and Y. Yue are with the Department of Computer Science and Software Engineering, Xi'an Jiaotong-Liverpool University, Suzhou, 215123 China e-mail: {Ziqiang.Bi, Jieming.Ma, Ka.Man, Yong.Yue}@xjtlu.edu.cn.

Z. Bi and J. S. Smith are with the Department of Electrical Engineering and Electronics, University of Liverpool, Liverpool, L69 3GJ, United Kingdom e-mail: J.S.Smith@liverpool.ac.uk.

H. Wen is with the Department of Electrical and Electronic Engineering, Xi'an Jiaotong-Liverpool University, Suzhou, 215123, China e-mail: Huiqing.Wen@xjtlu.edu.cn.

K. L. Man is also with the imec-DistriNet, KU Leuven, Leuven, B-3001, Belgium and the Faculty of Engineering, Computing and Science, Swinburne University of Technology Sarawak Campus, Kuching 93350, Malaysia.

Manuscript received April 19, 2005; revised August 26, 2015.

the voltage tuning process and makes the system simple. However, some regions are scanned repeatedly since overlaps exist between two adjacent scanning ranges. A modified IncCond method based on the idea of the $0.8V_{OC}$ model was proposed in [14]. A novel duty cycle computation method for tuning the operating voltage was introduced to improve the scanning speed. The search-skip-judge global MPPT (SSJ-GMPPT) method in [15] modifies the comparing procedure of the original $0.8V_{OC}$ model to avoid some unnecessary scanning processes under some specific shading scenarios. The rapid global MPPT (R-GMPPT) method in [15] introduces the current sensing circuit for estimating the approximate GMPP. Therefore, the tracking time of the R-GMPPT is significantly reduced by more than 90% compared to the traditional global searching method [15]. To obtain the peak power at each multiple of $0.8V_{OC}$ region, Aquib et al. [16] proposed an intelligent technique to compute the reference voltage value for the traditional P&O method. The GMPP is determined afterward by comparing each peak power. The $0.8V_{OC}$ model is capable of determining the GMPP under most shading patterns. However, one of the critical disadvantages of the aforementioned $0.8V_{OC}$-model-based approaches is that the tracking performance of the $0.8V_{OC}$ model is highly dependent on the length of the PV string [17]. More computation time is required on iteratively scanning the $0.8V_{OC}$ vicinities for longer PV strings.

Many GMPPT methods based on the metaheuristic optimization algorithms (e.g. Particle Swarm Optimization (PSO) [18], [19] and Ant Colony Optimization (ACO) [20]) have been proposed in the recent ten years to address the MPPT problems under partial shading conditions. According to the intrinsic properties of the optimization algorithms, these methods have the following two drawbacks. First, due to random sampling, the optimization-algorithm-based methods may get different prediction/tracking errors each time. Moreover, the optimization algorithms cannot guarantee that the global optimum can be obtained every time [21]. Sometimes these optimization-algorithm-based methods will be trapped in the local MPPs.

Shading information, such as the shading rate and shading strength, provides mathematical indicators for describing the PSC for PV strings. The shading rate χ expresses the percentage of the shaded PV modules [22] while the shading strength ρ reflects the ratio of received solar irradiance in a PV string [23]. The results in [22] have shown that the location of the GMPP is related to the value of the shading information. A shading detection method based on the electrical characteristics was proposed in [24] to estimate the shading rate. A GMPP estimation model based on the shading information was proposed in [25]. The voltage at the GMPP is estimated from the shading rate and the shading strength by the multiple Gaussian process regression (M-GPR) method with a mean absolute error (MAE) of 0.381 V under various PSC. In [17], a GMPPT method based on the detection of the shading rate was proposed. A mathematical relationship between the voltage at the GMPP and the shading rate was introduced based on the $0.8V_{OC}$ model. The performance of this method is not affected by the number of modules in the PV string. At the same time, the method saves around 50% of the tracking time by comparing with the traditional $0.8V_{OC}$-model-based methods for a PV string with three modules. These researches have shown that the location of the GMPP can be estimated from the shading information. However, the application area is limited since the existing shading rate and shading strength can only express the PSC with two irradiation levels according to their definitions [22].

To address the aforementioned problems, the improvements are proposed in this paper. The main contributions of this paper are as follows.

- A new form of the shading information, shading vector, is proposed to give a comprehensive expression for the shading conditions;
- A fast shading detection circuit is proposed to detect the shading vector;
- A novel $0.8V_{OC}$-model-based GMPPT method based on k-NN is proposed to improve the performance of the typical $0.8V_{OC}$-model-based methods for long PV strings.

The rest of the paper is organized as follows. Section II introduces the proposed shading vector and how to predict the GMPP from the shading vector. The structure of the proposed GMPPT method along with the detection circuit for the shading vector is illustrated in Section III. The simulation and experimental results are discussed in Section IV. Finally, Section V presents the conclusions of this paper.

II. Shading Vector and Global Maximum Power Point

A. Introduction of Shading Vector

The shading information is the mathematical indicator to quantitatively evaluate the PSC. The shading rate and shading strength are two typical forms of the shading information. According to [22], the definitions for both the shading rate and shading strength are based on a strong assumption. That is the PV string is supposed to be subjected to two different solar irradiation levels. The PV modules that receive the higher irradiance are called insolated modules, and those receiving the lower irradiance are called shaded modules. Thus, these two types of shading information are not compatible with the PSC with more than two irradiation levels. In this paper, the shading vector is proposed to comprehensively quantify the PSC.

Let γ denote the shading vector, which is defined as the union of the shading strength for the individual modules in the PV string. The shading vector is expressed as in (1).

$$\gamma = \bigcup_{i=1}^{N_{String}} \rho_i, \rho_i = \frac{G_i}{G_{Insolated}} \tag{1}$$

where ρ_i and G_i are respectively the shading strength and the solar irradiance of the ith PV module. $G_{Insolated}$ is the irradiance of the insolated or unshaded modules.

Each element in the shading vector represents the shading strength information for the corresponding PV module. The shading vector can also be used to reflect the number of shaded PV modules at each shading level. For example, a

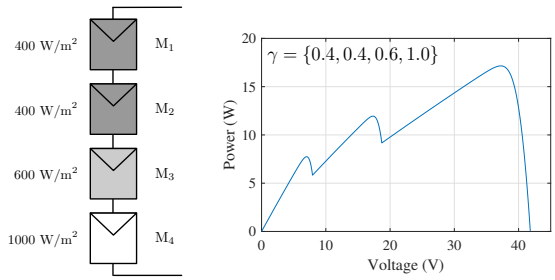

Fig. 1. An example of using the shading vector: (a) a PV string with four modules; (b) P-V curve of the PV string.

PV string with four modules is operating under PSC as shown in Fig. 1(a). The P-V curve with three peaks is shown in Fig. 1(b). The solar irradiance for four PV modules are 400, 400, 600, 1000 W/m^2, respectively. Thus, the shading vector under such shading conditions is {0.4, 0.4, 0.6, 1.0} according to the definition. Two elements with the same value 0.4 are inspected in the shading vector, as a result, two PV modules are receiving the same solar irradiation level. The rest two PV modules receive different irradiation levels as the elements in the shading vector are not the same. Therefore, multiple identical values in the shading vector indicate that the corresponding PV modules receive the same level of solar irradiance.

B. Determination of the Global Maximum Power Point

For a single PV module, the maximum power point (MPP) appears at the vicinity of $0.8\times V_{OC,M}$, where $V_{OC,M}$ is the open-circuit voltage of a single PV module. For a PV string, based on the 0.8V$_{\rm OC}$ model, the peak regions of the P-V curve are approximately at the multiples of $0.8\times V_{OC,M}$ and the GMPP is the peak region with the largest power.

The 0.8V$_{\rm OC}$-model-based MPPT method is a typical two-stage GMPPT method. At the first stage, the 0.8V$_{\rm OC}$ model determines the 0.8V$_{\rm OC}$ region with the largest power as the GMPP region by iteratively measuring and comparing the power at each 0.8V$_{\rm OC}$ region. At the second stage, the conventional MPPT technique (such as P&O and IncCond) is used to track the accurate GMPP. However, such measuring and comparing process takes a long time to get the GMPP region, especially for long PV strings. The efficiency of the 0.8V$_{\rm OC}$-model-based MPPT method can be improved by predicting the 0.8V$_{\rm OC}$ region with the GMPP from the extracted shading vector.

In order to have a clear illustration for the relationship between the 0.8V$_{\rm OC}$ region with the GMPP and the shading vector under various shading conditions, a PV string with three modules is used in the analysis. Fig. 2 shows the relationship between the 0.8V$_{\rm OC}$ region with the GMPP and three elements in the shading vector. Let n_{GMPP} denote the 0.8V$_{\rm OC}$ region with the GMPP, three shapes with different colors are used to distinguish the varied n_{GMPP} values. Fig. 2(a) is the three-dimension view of the data distribution. As the definition of the shading vector, at least one element in the shading vector is 1. Thus, all the data are distributed at the surface of a cubic.

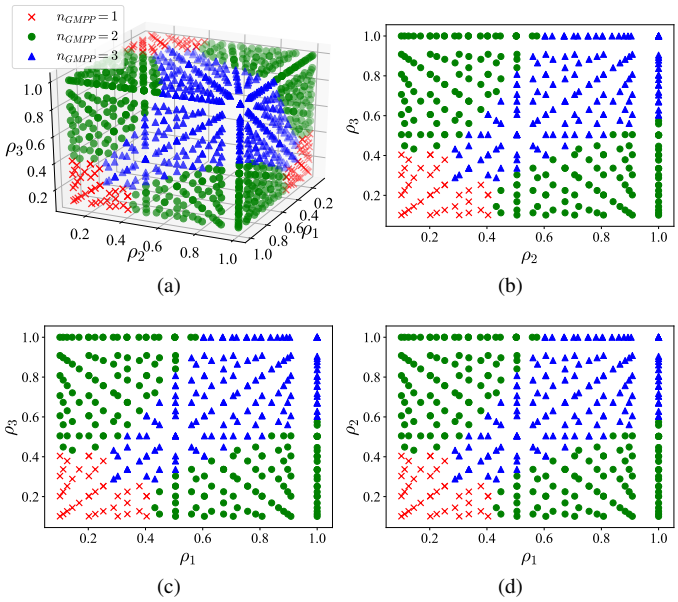

Fig. 2. The relationship between the n_{GMPP} and shading vector for a PV string with three modules under various shading conditions: (a) three-dimension view; (b) $\rho_1 = 1$; (c) $\rho_2 = 1$; (d) $\rho_3 = 1$.

Fig. 2(b) to 2(d) are views in three different directions. It is clearly observed that the data with different n_{GMPP} values are distributed in distinguished clusters. Therefore, the 0.8V$_{\rm OC}$ region with the GMPP n_{GMPP} can be predicted from the shading vector by classification algorithms.

In the proposed GMPPT method, the k-Nearest Neighbors (k-NN) classification algorithm [26] is used to predict the 0.8V$_{\rm OC}$ region with the GMPP. k-NN classification algorithm is widely applied in the Internet of Things (IoT) [27], wireless sensor networks (WSN) [28], electric vehicles [29] and many other scenarios. The inputs of the k-NN classifier are the elements in the shading vector. As a result, the size of the input of the k-NN classifier is dependent on the number of PV modules in the string. PV strings with different lengths need varied classifiers. The output of the k-NN classifier is the 0.8V$_{\rm OC}$ region with the GMPP n_{GMPP}.

Assuming that the temperature is evenly distributed for all the PV modules in the PV string, the open-circuit voltage for each module is identical. According to the theory of the 0.8V$_{\rm OC}$ model, the GMPP exists at multiples of $0.8\times V_{OC,M}$. With the knowledge of the 0.8V$_{\rm OC}$ region with the GMPP n_{GMPP}, the voltage at the GMPP can be estimated by (2).

$$V_{GMPP} \approx 0.8 \times V_{OC,M} \times n_{GMPP} \tag{2}$$

where $V_{OC,M}$ is the open-circuit voltage of a single module, which can be estimated from the value under STC by (3) [30].

$$V_{OC,M} = V_{OC,M,STC} + K_V \Delta T \tag{3}$$

where K_V is the open-circuit voltage temperature co-efficient.

III. Proposed Global Maximum Power Point Tracking Method

A. Detection of the Shading Vector

The shading vector is critical for predicting the position of the GMPP. The detection of the shading vector is the first step to obtain the $0.8V_{OC}$ region with the GMPP.

The relationship between the short-circuit current I_{SC} and the solar irradiance G for a single PV module is given in (4) [30].

$$I_{SC} = (I_{SC,STC} + K_I \Delta T)\frac{G}{G_{STC}} \tag{4}$$

where $I_{SC,STC}$ is the short-circuit current at the standard test condition (STC, 25 °C and 1000 W/m^2); K_I the short-circuit current temperature co-efficient; $\Delta T = T - T_{STC}$ the temperature difference between the actual ambient temperature and the reference temperature at STC; G_{STC} the reference solar irradiance at STC. The value of $I_{SC,STC}$ and K_I can be found in the datasheet of the PV modules. When the temperature is fixed, the value of the short-circuit current I_{SC} is proportional to the value of the solar irradiance G. Thus, the ratio of the solar irradiance can be estimated by measuring the ratio of the short-circuit currents.

Fig. 3 analyzes the current characteristics of a PV string with three modules. The PV string as shown in Fig. 3(a) is operating under PSC. Fig. 3(b) to 3(d) record the current of the PV modules and the bypass diodes across the whole string voltage range. It can be observed that when the whole PV string is short-circuited, the individual PV modules are generating the maximum current they can produce under each solar irradiation condition. The summation of the current from the PV module and its bypass diode is the string current. Therefore, Only the short-circuit point of the PV string is needed to measure the short-circuit currents for all the PV modules.

According to the current characteristics, the current sensors are used for all the PV modules to detect the shading strength vector. The block diagram of the shading detection circuit for the shading vector is shown in Fig. 4. The current sensor is connected in series with each PV module to measure the module current. The detection procedure is described in Algorithm 1.

In the beginning, the current operating status is saved by recording the operating string voltage V_{OP}. To measure the short-circuit current, the PV string is going to operate at the short-circuit point. The currents at the string voltage of $10\% \times V_{OC,M}$ are collected as the short-circuit currents $\boldsymbol{I_{SC}}$ $(I_{SC,1}, \ldots, I_{SC,N_{String}})$ to avoid the PV string from being totally short-circuited. Then, the operating string voltage is adjusted to the saved V_{OP}. The largest current is selected as the short-circuit current of the insolated module $I_{SC,Insolated}$. Finally, the shading vector is obtained by (5).

$$\gamma = \bigcup_{i=1}^{N_{String}} \frac{I_{SC,i}}{I_{SC,Insolated}} \tag{5}$$

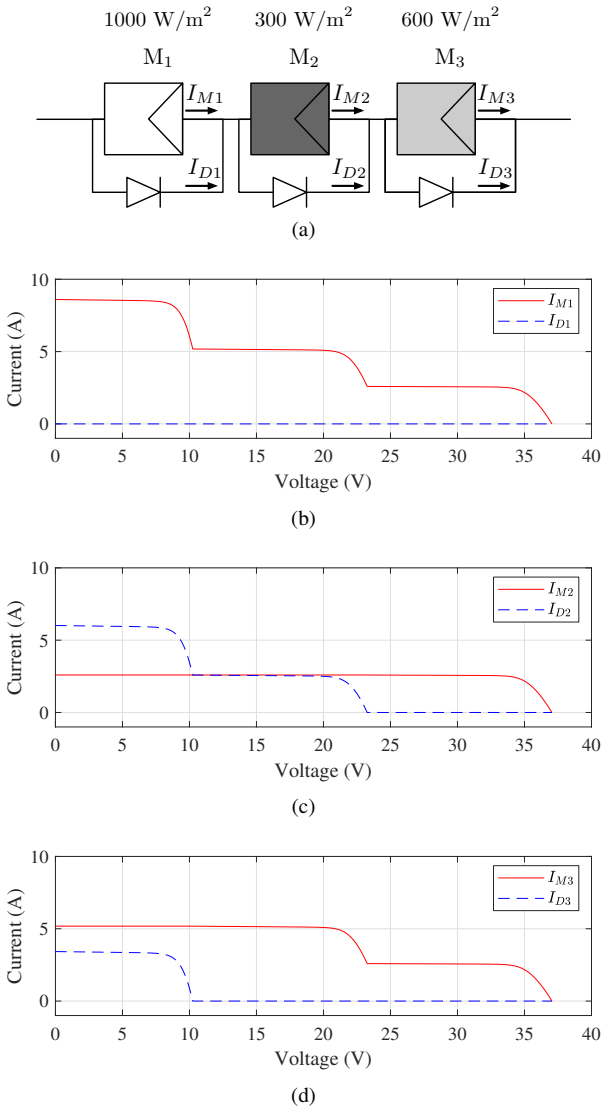

Fig. 3. Current characteristics of PV modules and bypass diodes in the PV string under PSC: (a) the block diagram; (b) module 1; (c) module 2 and (d) module 3.

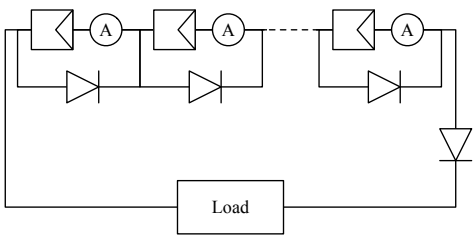

Fig. 4. Shading detection circuit for the shading vector.

B. Overview of the Proposed Method

Fig. 5 depicts the block diagram of the proposed GMPPT method. The shading vector is detected by the shading detection circuit integrated in the PV string. The ambient temperature is collected by the thermometer to adjust the module open-circuit voltage by (3). The microcontroller obtains the detected shading vector and gets the predictions of the n_{GMPP} by k-NN. The operating voltage of the PV string is adjusted

Algorithm 1 The procedure for the shading detection circuit.

Input: the number of PV modules in the PV string N_{String}
Output: the shading vector γ

1: Record the current operating voltage V_{OP}.
2: Adjust the string voltage to $10\% \times V_{OC,M}$.
3: Collect the value of each current sensor $\boldsymbol{I_{SC}}$.
4: Adjust the operating voltage to the recorded V_{OP}.
5: $I_{SC,Insolated} \leftarrow$ the largest current in $\boldsymbol{I_{SC}}$.
6: Obtain the shading vector by (5).

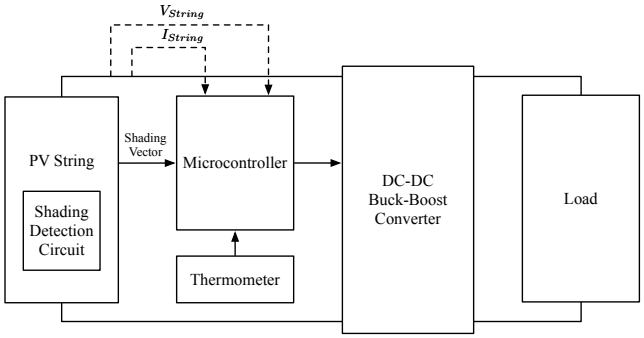

Fig. 5. Block diagram of the proposed GMPPT method.

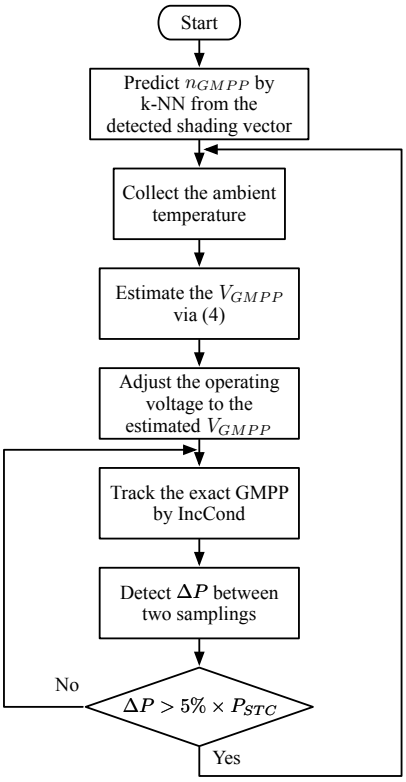

Fig. 6. Flowchart of the proposed GMPPT method.

to the estimated V_{GMPP} from (2) by controlling the DC-DC converter.

The flowchart of the proposed GMPPT method is given in Fig. 6. Firstly, the $0.8V_{OC}$ region with the GMPP n_{GMPP} is predicted by k-NN classification algorithm from the detected shading vector. The ambient temperature is collected and the voltage at the GMPP V_{GMPP} is estimated by (2). After tuning the operating voltage to the estimated V_{GMPP}, the traditional MPPT scheme IncCond is finally used to track the exact GMPP. The power difference ΔP between two adjacent samplings is detected continuously at a fixed frequency (depends on the step of IncCond). The shading pattern is assumed as changed when the power difference ΔP is larger than $5\% \times P_{STC}$. At the same time, the proposed tracking method is rolled back to the initial state and a new V_{GMPP} is predicted.

IV. Results and Discussions

A. Simulation Results

Three datasets for PV strings with 3, 4 and 5 modules under various shading patterns are generated in MATLAB/Simulink 2019b. The specification of the used PV module is listed in TABLE I. To verify the prediction performance of k-NN classification algorithm in the proposed GMPPT method, four popular classification algorithms including logistic regression (LR), Gaussian naive bayes (GNB), artificial neural network (ANN) and support vector machine (SVM) are introduced into the comparison study. The classification tools from scikit-learn [31] are used to assess the three algorithms on the generated datasets. The comparison results as shown in TABLE II are the average accuracy from the three classification algorithms based on the 100 times of 10-fold cross-validation.

TABLE I
Specifications of the PV module used in this research under standard test condition.

Parameters	Variable	Value	Unit
Short-circuit current	I_{SC}	1.23	A
Open-circuit voltage	V_{OC}	10.71	V
Current at MPP	I_{MPP}	1.12	A
Voltage at MPP	V_{MPP}	9.00	V
Maximum power	P_{MPP}	10.00	W
Temperature co-effcient of I_{SC}	K_I	0.062	A/°C
Temperature co-effcient of V_{OC}	K_V	-0.080	V/°C

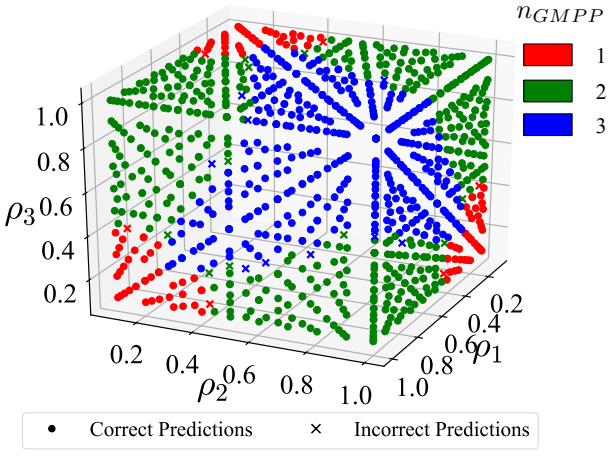

Fig. 7. Visualization for the classification results (N_{String} = 3, k = 20).

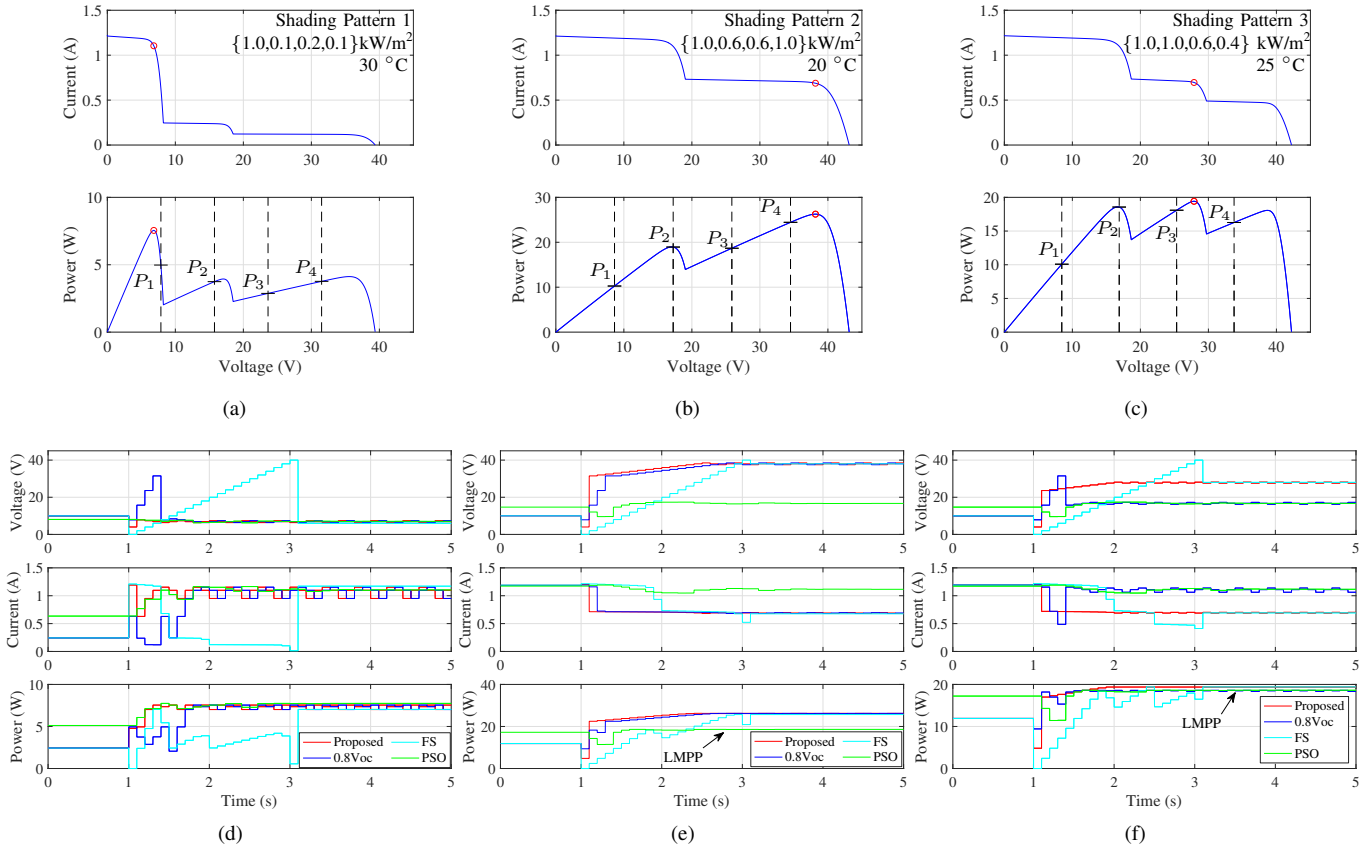

Fig. 8. Simulated tracking results for a PV string with four modules under three fixed shading patterns: (a) PV characteristics and (d) tracking results under shading pattern 1; (b) PV characteristics and (e) tracking results under shading pattern 2; (c) PV characteristics and (f) tracking results under shading pattern 3.

TABLE II
AVERAGE CLASSIFICATION ACCURACY FROM DIFFERENT CLASSIFICATION ALGORITHMS BASED ON 100 TIMES OF 10-FOLD CROSS-VALIDATION.

N_{String} (Size of dataset)	3 (10^3)	4 (10^4)	5 (10^5)
k-Nearest Neighbors (k=20)	97.00%	96.05%	95.14%
Logistic Regression	71.57%	54.23%	44.52%
Gaussian Naive Bayes	70.76%	59.78%	50.39%
Artificial Neural Network	62.39%	56.10%	46.70%
Support Vector Machine	79.16%	68.40%	60.42%

The sizes of three datasets are respectively 1,000, 10,000 and 100,000. The increment in the size of the dataset has a huge impact on the average accuracy for the classification algorithms except for the k-NN. The average accuracy values for LR, GNB, ANN and SVM are getting lower with the increasing size of the dataset. However, the average accuracy for the k-NN classifier is above 95% for all three datasets in the comparison test. Thus, the comparison study has shown that the k-NN algorithm has a better performance in classifying the $0.8V_{OC}$ region with the GMPP.

Fig. 7 visualizes the classification results for PV strings with three modules. Different colors are used to distinguish different prediction labels. The solid circles are the correct predictions, while the crosses are the incorrect predictions. It can be found from the distribution results that the incorrect predictions are located at the intersections between different classes, where the power between two MPP regions are close to each other.

The performance of the proposed GMPPT method is compared with the traditional $0.8V_{OC}$-model-based method, the full scanning (FS) method in [6] and the particle swarm optimization (PSO)-based method in [18]. The simulation was implemented with a PV string with four modules under three varied shading patterns. The specification of the used PV module is the same and listed in TABLE I. The parameter setting of PSO-based method was referred to [18], where the inertia weight ω = 0.4; acceleration coefficients c_1 = 1.2 and c_2 = 1.6. The simulated tracking results are shown in Fig. 8, where Fig. 8(a), 8(b) and 8(c) depict the PV characteristics for the three shading patterns. The power at multiples of $0.8\times V_{OC,M}$ (black vertical dash-lines in P-V curves) are labeled as P_1, P_2, P_3 and P_4. The corresponding comparison results between four GMPPT methods are shown in Fig. 8(d), 8(e) and 8(f).

All the involved GMPPT methods were activated at 1 s and the controlling step was 0.1 s. The voltage scanning step for the full scanning method was set to 2 V. When starting tracking, the proposed GMPPT method detects the shading vector by adjusting the string voltage to the measuring point. The traditional $0.8V_{OC}$-model-based method iteratively

measures the power values at multiples of $0.8\times V_{OC,M}$ point. For all three shading patterns, the proposed method finishes detecting the shading vector and obtains the predictions by one step, while the traditional $0.8V_{OC}$-model-based method finishes comparing process with 4 steps. Based on the current simulation setup, the proposed method reduces the tracking step by 75% compared with the traditional $0.8V_{OC}$-model-based method. The scanning time of the full scanning method is highly dependent on the voltage scanning step. Under the current voltage scanning step of 2 V, it takes 2.1 s for the full scanning method to finish the voltage scanning for all three shading patterns. Such scanning time is much longer than the time for reaching the GMPP by the proposed method. Moreover, since the voltage scanning step is quite large, under the shading pattern 1 and 2, the final tracked powers of the full scanning method are lower than the real GMPPs. Furthermore, the performance of the traditional $0.8V_{OC}$-model-based method is dependent on the string length. It takes more steps to get the $0.8V_{OC}$ region with the GMPP for the traditional $0.8V_{OC}$-model-based method when applying on a longer PV string. The performance of the proposed GMPPT method is not affected by the string length since the detection of the shading vector is executed in parallel.

Under shading patterns 2 and 3, the PSO-based method fails to track the GMPP and is trapped in the local peaks. It usually takes around 0.8 s for the PSO-based method to reach a solution with small oscillations. Although the tracking speed of the PSO-based method is sometimes faster than the proposed method, it cannot guarantee that the GMPP can always be tracked.

As can be seen from the P-V curves, the peak power points are not always existing at the multiples of $0.8\times V_{OC,M}$. In shading pattern 3, the power at the second $0.8V_{OC}$ point P_2 (LMPP) is larger than the third one P_3 (GMPP). As a result, the traditional $0.8V_{OC}$-model-based method does not track the global maximum in shading pattern 3. This problem does not influence the prediction of the proposed method as the trained dataset has the correct $0.8V_{OC}$ region with the GMPP.

B. Experimental Results

A PV string with four PV modules was used to validate the effectiveness of the proposed GMPPT method. The setup of the hardware implementation is shown in Fig. 9. The four PV modules have the same specification to the PV module used in the simulation. In order to make the PV string operate under stable partial shading conditions, some floodlights with Halogen lamps were used to emulate the sunlight in the indoor environment. The ambient temperature was captured by the thermometer (DS18B20) attached at the rear of the PV module. The sensor module (JSY-MK-218) was used to measure the string voltage, string current and the current of each PV module. The microcontroller (UDOO NEO) implements the shading detection and the proposed GMPPT algorithms. The oscilloscope (GW Instek GDS-2202A) was used to record the tracking results by voltage and current probes. The operating point of the PV string is adjusted by a DC-DC buck-boost converter (ANHE BB4805S) and an electronic load (ITECH IT8512A+) with the fixed resistance.

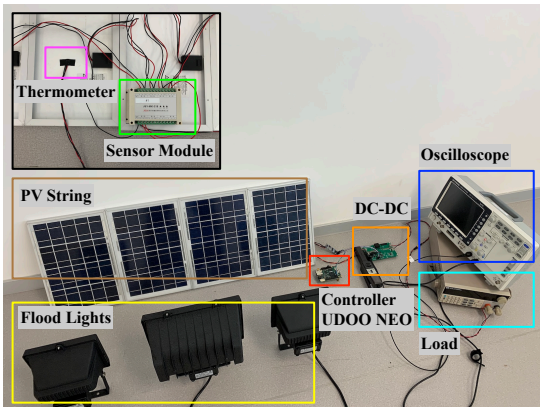

Fig. 9. Hardware setup of the experimental implementation.

The experimental results show the tracking performance of the proposed GMPPT method under the fixed partial shading conditions and changing shading patterns.

1) Fixed Shading Conditions: Three partial shading conditions are emulated in this section. The ambient temperature is around 25 °C in the indoor environment. The positions of the floodlights and the PV modules are as shown in Fig. 10(a), 10(d) and 10(g). The power of each floodlight and the distances between the lights and the PV modules are labeled on the figures.

For each shading pattern, the currents and voltages were measured by scanning the string voltage from 0 V to the string open-circuit voltage in order to acquire the I-V characteristics. The power information was calculated from the measured current and voltage data. The I-V and P-V characteristics under each PSC were drawn in MATLAB as shown in Fig. 10(b), 10(e) and 10(h). The GMPPs are marked by the red circles on the I-V curves and P-V curves. Under three PSCs, the GMPPs are respectively distributed at the $0.8V_{OC}$ regions 2, 3 and 4. The corresponding voltage and current values at the GMPP are listed near the GMPP on each I-V curve.

Fig. 10(c), 10(f) and 10(i) are the tracking results captured by the oscilloscope. The string voltage and current are recorded as the yellow and blue curves. The red curve is the string power generated by the production function of the oscilloscope. When the tracking algorithm is activated, it can be observed that the string voltage is tuned to a lower value to detect the shading vector. For all three PSCs, the $0.8V_{OC}$ region with the GMPP is correctly predicted and the operating point is adjusted to the predicted value after finishing the shading detection process. Then, the traditional MPPT method IncCond is used to track the exact GMPP.

2) Changing Shading Conditions: When using the IncCond method to track the exact GMPP, the proposed GMPPT method continuously detects the power difference between two data samplings in case that there is a sudden change in the shading pattern. In this test, the shading pattern was suddenly changed when the system was operating at a steady state to verify the effectiveness of the proposed GMPPT method under changing shading conditions. The string power at STC P_{STC} for the current setup is 40 W, and as a result, the threshold is set to $5\%\times P_{STC}$ = 2 W.

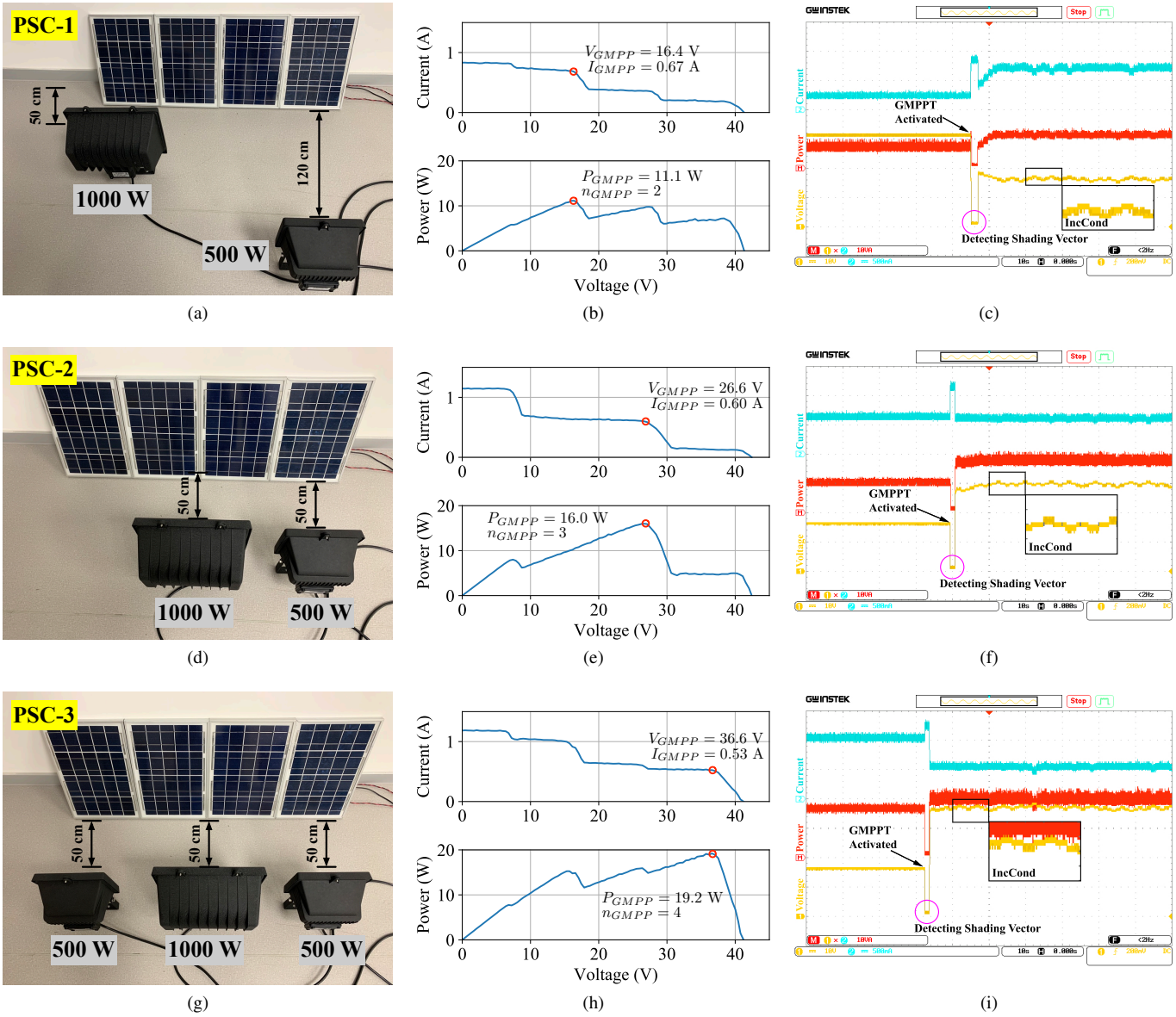

Fig. 10. Experimental results of the proposed GMPPT method under fixed partial shading conditions. The top row: (a) light position, (b) scanned PV characteristic curves and (c) tracking results under PSC-1; the middle row: (d) light position, (e) scanned PV characteristic curves and (f) tracking results under PSC-2; the bottom row: (g) light position, (h) scanned PV characteristic curves and (i) tracking results under PSC-3.

Fig. 11 shows the tracking results under changing shading conditions. PSC-2 and PSC-3 used in the test under fixed shading conditions are involved in this experiment. The shading pattern is initially set to PSC-3, the proposed GMPPT method successfully tracks the GMPP under PSC-3 after the method is activated. When the string power was optimized by the IncCond, the shading pattern was suddenly changed to PSC-2. As the detected power difference ΔP was greater than 2 W, the shading detection algorithm was activated again to update the shading vector. The new prediction was generated based on the updated shading vector.

Under both shading patterns, the locations of the GMPP are correctly predicted by the proposed GMPPT method. The proposed GMPPT method is capable of tracking the GMPP under the rapidly changing partial shading conditions.

V. Conclusions

In this paper, an enhanced $0.8V_{OC}$-model-based method has been proposed to track the GMPP for a PV string under the PSC. To locate the GMPP based on the shading characteristics, the shading vector is proposed to express the shading patterns. A fast shading detection method has been proposed to identify the shading vector. The k-NN classification algorithm is applied to predict the $0.8V_{OC}$ region with the GMPP from the identified shading vector.

The simulations and hardware experiments have been conducted to verify the effectiveness of the proposed GMPPT method. The k-NN algorithm has been validated to have an accuracy of around 96% when predicting the $0.8V_{OC}$ region with the GMPP. A comparative study has been conducted among the proposed method, the traditional $0.8V_{OC}$-model-

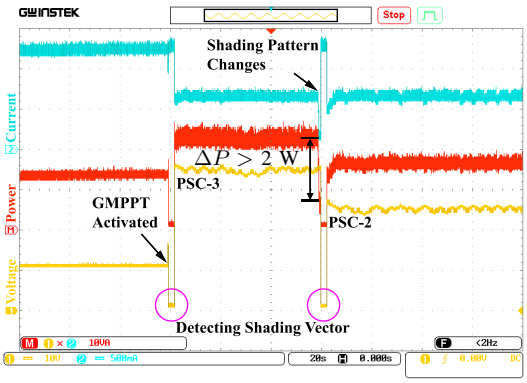

Fig. 11. Tracking results of the proposed under changing partial shading conditions (changing from PSC-3 to PSC-2).

based method, the full scanning method, and the PSO-based method. By comparing with the traditional $0.8V_{OC}$-model-based GMPPT method, the simulation results have shown that the proposed GMPPT method reduces the tracking step by 75% for a PV string with four modules.

ACKNOWLEDGMENT

This research is supported by the Natural Science Foundation of China (Grant No. 61702353), the Suzhou Science and Technology Project-Key Industrial Technology Innovation (Grant No. SYG201841), Qing Lan Project of Jiangsu Province, the Open Foundation of the Suzhou Smart City Research Institute, Suzhou University of Science and Technology, the Key Program Special Fund of Xi'an Jiaotong-Liverpool University (XJTLU), Suzhou, China (Grant No. KSF-P-02, KSF-E-65), and the Research Development Fund of XJTLU (Grant No. RDF-14-02-32, RDF-17-02-04).

REFERENCES

[1] S. Mekhilef, R. Saidur, and A. Safari, "A review on solar energy use in industries," *Renewable Sustainable Energy Rev.*, vol. 15, no. 4, pp. 1777 – 1790, 2011.

[2] J. C. Teo, R. H. G. Tan, V. H. Mok, V. K. Ramachandaramurthy, and C. Tan, "Impact of partial shading on the P-V characteristics and the maximum power of a photovoltaic string," *Energies*, vol. 11, no. 7, 2018.

[3] N. Femia, G. Petrone, G. Spagnuolo, and M. Vitelli, "Optimization of perturb and observe maximum power point tracking method," *IEEE Trans. Power Electron.*, vol. 20, no. 4, pp. 963–973, July 2005.

[4] M. A. Elgendy, B. Zahawi, and D. J. Atkinson, "Assessment of the incremental conductance maximum power point tracking algorithm," *IEEE Trans. Sustain. Energy*, vol. 4, no. 1, pp. 108–117, Jan 2013.

[5] M. E. Başoğlu, "An improved 0.8 Voc model based GMPPT technique for module level photovoltaic power optimizers," *IEEE Trans. Ind. Appl.*, vol. 55, no. 2, pp. 1913–1921, March 2019.

[6] E. Koutroulis and F. Blaabjerg, "A new technique for tracking the global maximum power point of PV arrays operating under partial-shading conditions," *IEEE J. Photovolt.*, vol. 2, no. 2, pp. 184–190, April 2012.

[7] H. Patel and V. Agarwal, "Maximum power point tracking scheme for PV systems operating under partially shaded conditions," *IEEE Trans. Ind. Electron.*, vol. 55, no. 4, pp. 1689–1698, April 2008.

[8] A. Kouchaki, H. Iman-Eini, and B. Asaei, "A new maximum power point tracking strategy for PV arrays under uniform and non-uniform insolation conditions," *Sol. Energy*, vol. 91, pp. 221 – 232, 2013.

[9] M. E. Başoğlu and B. Çakir, "Experimental evaluations of global maximum power point tracking approaches in partial shading conditions," in *17th IEEE Int. Conf. on Environ. Elect. Eng., 1st IEEE Ind. Commercial Power Syst. Eur. (EEEIC / I CPS Eur.)*, Milan, Italy, June 2017, pp. 1–5.

[10] M. E. Başoğlu and B. Çakır, "Hybrid global maximum power point tracking approach for photovoltaic power optimisers," *IET Renewable Power Gener.*, vol. 12, pp. 875–882(7), June 2018.

[11] K. Chen, S. Tian, Y. Cheng, and L. Bai, "An improved MPPT controller for photovoltaic system under partial shading condition," *IEEE Trans. Sustain. Energy*, vol. 5, no. 3, pp. 978–985, July 2014.

[12] M. E. Başoğlu, "A fast GMPPT algorithm based on PV characteristic for partial shading conditions," *Electronics*, vol. 8, no. 10, 2019.

[13] ——, "An enhanced scanning-based MPPT approach for DMPPT systems," *Int. J. Electron.*, vol. 105, no. 12, pp. 2066–2081, 2018.

[14] K. S. Tey and S. Mekhilef, "Modified incremental conductance algorithm for photovoltaic system under partial shading conditions and load variation," *IEEE Trans. Ind. Electron.*, vol. 61, no. 10, pp. 5384–5392, Oct 2014.

[15] Y. Wang, Y. Li, and X. Ruan, "High-accuracy and fast-speed MPPT methods for PV string under partially shaded conditions," *IEEE Trans. Ind. Electron.*, vol. 63, no. 1, pp. 235–245, Jan 2016.

[16] M. Aquib, S. Jain, and V. Agarwal, "A time-based global maximum power point tracking technique for PV system," *IEEE Trans. Power Electron.*, pp. 1–1, 2019.

[17] Z. Bi, J. Ma, K. L. Man, J. S. Smith, Y. Yue, and H. Wen, "Global MPPT method for photovoltaic systems operating under partial shading conditions using the 0.8Voc model," in *19th IEEE Int. Conf. on Environ. Elect. Eng., 3rd IEEE Ind. Commercial Power Syst. Eur. (EEEIC / I CPS Eur.)*, Genova, Italy, June 2019, pp. 1–6.

[18] K. Ishaque, Z. Salam, M. Amjad, and S. Mekhilef, "An improved particle swarm optimization (PSO)–based MPPT for PV with reduced steady-state oscillation," vol. 27, no. 8, pp. 3627–3638, Aug. 2012.

[19] K. Ishaque and Z. Salam, "A deterministic particle swarm optimization maximum power point tracker for photovoltaic system under partial shading condition," vol. 60, no. 8, pp. 3195–3206, Aug. 2013.

[20] S. Titri, C. Larbes, K. Y. Toumi, and K. Benatchba, "A new mppt controller based on the ant colony optimization algorithm for photovoltaic systems under partial shading conditions," *Applied Soft Computing*, vol. 58, pp. 465 – 479, 2017. [Online]. Available: http://www.sciencedirect.com/science/article/pii/S1568494617302703

[21] Guiying Li and Zhigang Yu, "The double chaotic particle swarm optimization with the performance avoiding local optimum," in *2015 International Conference on Estimation, Detection and Information Fusion (ICEDIF)*, 2015, pp. 424–427.

[22] J. Ma, X. Pan, K. L. Man, X. Li, H. Wen, and T. On Ting, "Detection and assessment of partial shading scenarios on photovoltaic strings," *IEEE Trans. Ind. Appl.*, vol. 54, no. 6, pp. 6279–6289, Nov 2018.

[23] F. Salem and M. A. Awadallah, "Detection and assessment of partial shading in photovoltaic arrays," *J. Electr. Syst. Inf. Technol.*, vol. 3, no. 1, pp. 23 – 32, 2016.

[24] J. Ma, Z. Bi, K. L. Man, Y. Yue, and J. S. Smith, "Automatic shading detection system for photovoltaic strings," in *2018 Int. SoC Design Conf. (ISOCC)*, Daegu, Korea (South), Nov 2018, pp. 176–177.

[25] J. Ma, Z. Bi, K. L. Man, H. Liang, and J. S. Smith, "Predicting the global maximum power point locus using shading information," in *19th IEEE Int. Conf. on Environ. Elect. Eng., 3rd IEEE Ind. Commercial Power Syst. Eur. (EEEIC / I CPS Eur.)*, Genova, Italy, June 2019, pp. 1–5.

[26] N. S. Altman, "An introduction to kernel and nearest-neighbor nonparametric regression," *The American Statistician*, vol. 46, no. 3, pp. 175–185, 1992.

[27] M. I. AlHajri, N. T. Ali, and R. M. Shubair, "Classification of indoor environments for iot applications: A machine learning approach," *IEEE Antennas Wireless Propag. Lett.*, vol. 17, no. 12, pp. 2164–2168, Dec 2018.

[28] M. Xie, J. Hu, S. Han, and H. Chen, "Scalable hypergrid k-NN-based online anomaly detection in wireless sensor networks," *IEEE Trans. Parallel Distrib. Syst.*, vol. 24, no. 8, pp. 1661–1670, Aug 2013.

[29] Y. Hu, L. Yang, B. Yan, T. Yan, and P. Ma, "An online rolling optimal control strategy for commuter hybrid electric vehicles based on driving condition learning and prediction," *IEEE Trans. Veh. Technol.*, vol. 65, no. 6, pp. 4312–4327, June 2016.

[30] M. G. Villalva, J. R. Gazoli, and E. R. Filho, "Comprehensive approach to modeling and simulation of photovoltaic arrays," *IEEE Trans. Power Electron.*, vol. 24, no. 5, pp. 1198–1208, May 2009.

[31] F. Pedregosa, G. Varoquaux, A. Gramfort, V. Michel, B. Thirion, O. Grisel, M. Blondel, P. Prettenhofer, R. Weiss, V. Dubourg, J. Vanderplas, A. Passos, D. Cournapeau, M. Brucher, M. Perrot, and E. Duchesnay, "Scikit-learn: Machine learning in Python," *Journal of Machine Learning Research*, vol. 12, pp. 2825–2830, 2011.